Orthogonal Resonators for Circularly Polarized Filtering Antenna Using a Single Feedline

Dwi Astuti Cahyasiwi, *Member, IEEE*, Fitri Yuli Zulkifli, *Senior Member, IEEE*, and Eko Tjipto Rahardjo, *Member, IEEE*

***Abstract*— Polarization diversity is an antenna feature that has been widely researched to increase the capacity of a wireless communication system. The conceptual theory of polarization states that all polarization vectors can be decomposed into two orthogonal electric field vector modes. This study proposes a novel framework to bridge the gap between circular polarization (CP) technique and filtering antenna design using two orthogonal resonators with the ability to represent any polarization. The proposed method combines the techniques of antenna–filter and CP design into a single integrated step. To achieve the second-order antenna–filter integration and generate CP, the two orthogonal resonators modeled as a rectangular radiator and a $\lambda/4$ resonator combined. The CP filtering antenna operates at a frequency of 4.65 GHz, with an impedance bandwidth of 4.7%, an axial ratio (AR) bandwidth of 3.2%, and a gain of 6.2-dBi. To validate the CP filtering antenna, simulations and measurements were performed, and the results were found to be in good agreement.**

***Index Terms*— Circular polarization (CP), filtering antenna, interdigital, orthogonal resonator.**

I. Introduction

CIRCULARLY polarized antennas have been developed using various methods. The main principle that distinguishes antennas with linear and circular polarization (CP) is the ±90° phase difference between two orthogonal magnetic fields. Some techniques for generating CP have been studied [1], [2]. A single feed technique intervenes the radiator to create two electromagnetic field modes with a 90° phase delay. This technique can be achieved using truncated and perturbation radiator elements [2], [3], [4], [5], [6], [7], [8], [9], [10], [11], [12], [13], [14]. The simplest method to achieve two orthogonal modes is to insert two orthogonal feeders [15], [16], [17], [18]. However, as previously stated, two equal orthogonal fields will only generate CP if there is a 90° phase difference, so this technique requires an additional phase delay circuit. The cancellation circuits to generate delay have been reported in [19], [20], [21], [22], [23], [24], [25], and [26], and some of the circuits have been applied to obtain CP [18], [27].

The integration of a filter and antenna known as filtering antenna is advanced because of its controllable bandwidth impedance. Furthermore, it performs a frequency selectivity with its bandpass-like response gain. The most common method to design a filtering antenna is to create a filter network using a radiator and resonator. In a codesign technique, the antenna replaces the last stage resonator of the filter. CP filtering antennas have been studied using a single feedline [3], [4] and two orthogonal feedlines [17], [28], [29]. A truncated radiator generates CP, and a filtering circuit is added to provide selectivity features [3].

The filtering antennas create two orthogonal feedlines and 90° a phase delay circuit using a $\lambda/4$, $\lambda/2$, and two parallel $\lambda/2$ stub resonators [17], [28], [29]. Dispersive delay lines are added to one of the two orthogonal feedlines to obtain a circularly polarized filtering antenna [18]; their function is as filtering and delay circuits. All the extra components and two-step designs in the previous studies result in a bulky circuit.

In our previous studies, we developed 75°, 45°, and vertical polarization filtering antenna using the $\lambda/4$ resonator and a rectangular radiator [30], [31], [32]. In [31], the interaction between the radiator and resonator stimulates a second mode on the radiator and results in two orthogonal modes with a single feedline; in addition, with proper radiator size, 0° and 180° phase delay using a cancellation circuit in [22], the design generated 45° polarization. Based on the common characteristics of 45° polarization and CP, a circularly polarized antenna with a similar structure as in [31] can be designed by adding 90° phase delay. To the best of our knowledge, no technique on filtering antenna that uses its integration process to generate CP has been reported. Therefore, this study proposes a technique for designing a circularly polarized filtering antenna using single feedline that provides two orthogonal modes and 90° delay without an additional circuit or radiator perturbation. The proposed technique simplifies the design process of CP filtering antenna from two steps to one step. This method merges the antenna–filter integration and polarization generator technique. Furthermore, it applies to generate linear and CP. Characteristics of CP are proven with $|E_\theta|/|E_\Phi|$, phase difference (δ_L), and axial ratio (AR)

Manuscript received 30 September 2022; revised 18 December 2022; accepted 20 March 2023. Date of publication 27 April 2023; date of current version 5 October 2023. This work was supported in part by the Seed Funding Professor "under Grant NKB-1938/UN2.F4.D/PPM.00.00/2022." *(Corresponding author: Eko Tjipto Rahardjo.)*

Dwi Astuti Cahyasiwi is with the Electrical Engineering Department, Universitas Muhammadiyah Prof. Dr. HAMKA, South Jakarta 12130, Indonesia (e-mail: dwi.cahyasiwi@uhamka.ac.id).

Fitri Yuli Zulkifli and Eko Tjipto Rahardjo are with the Antenna and Microwave Research Group (AMRG), Electrical Engineering Department, Faculty of Engineering, Universitas Indonesia, Depok 16424, Indonesia (e-mail: eko@eng.ui.ac.id).

Color versions of one or more figures in this article are available at https://doi.org/10.1109/TMTT.2023.3267559.

Digital Object Identifier 10.1109/TMTT.2023.3267559

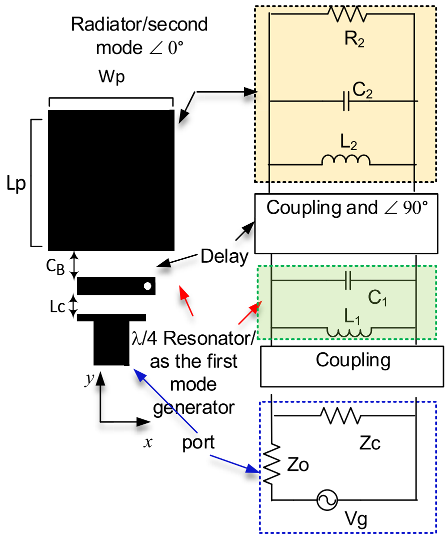

Fig. 1. Concept of the proposed antenna and its equivalent circuit.

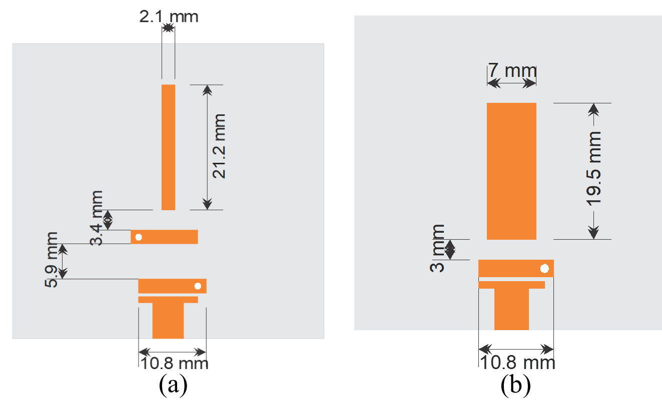

Fig. 2. Impure vertical polarization filtering antenna based on (a) third- and (b) second-order filter [32].

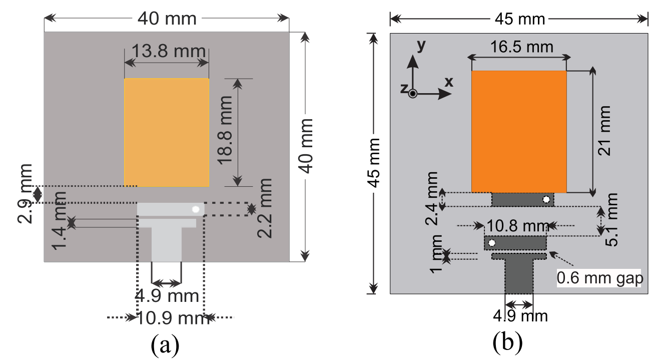

Fig. 3. (a) Impure 75° slant polarization [30] and (b) 45° polarization [31].

parameters, within the bandwidth operational. Selectivity performance is represented by the gain over the operational bandwidth. This article is organized as follows. Section II explains the proposed method for CP excitation using two orthogonal resonators based on the general polarization theory. Section III describes the antenna–filter integration. Section IV presents the result and discussion. Finally, the results are concluded in Section V.

II. Proposed Method

Polarization is a relation of the electrical fields in θ and Φ in the spherical coordinate system, as expressed in the following equation:

$$\bar{E} = E_{\theta}\cos(\omega t)\hat{\boldsymbol{\theta}} + E_{\Phi}\cos(\omega t + \delta_{\mathrm{L}})\hat{\Phi} \quad (1)$$

which explicates that the total electrical field, $\bar{E}$, can be decomposed into two virtual orthogonal electrical field vectors in $\hat{\theta}$ (E_{θ}) and $\hat{\phi}$ (E_{Φ}) directions [33]. Any polarization can be represented by two orthogonal linear polarizations (E_{θ} and E_{Φ}). In general, the magnitudes of these fields can be different or equal, and they may be in-phase or out of phase by an angle δ_{L}. If δ_{L} is 0° or 180°, it is linear, whereas, if δ_{L} is +90° or −90°, it is circular. Hence, from the theoretical framework above, these two virtual orthogonal electrical fields can be realized, with two individual structures represented by vertical and horizontal surface currents

$$|E_{\theta}| = |E_{\Phi}|. \quad (2)$$

The physical construction of the proposed method can be represented using the two orthogonal resonant structures as shown in Fig. 1, where an $\lambda/4$ resonator (L_1, C_1) represents e-field in the $\hat{\theta}$-direction, with a horizontal surface current along the x-axis to excite the second mode on the radiator, which is orthogonal to the radiator surface current. The gap between the $\lambda/4$ resonator and the radiator offers a 90° phase delay in addition to coupling between the resonator and the rectangular radiator. Using this gap, no additional delay circuit is required. The radiator (L_2, C_2, and R_2) represents the e-field in the $\hat{\phi}$-direction, with vertical surface current along the $y-$ axis. The gap between the $\lambda/4$ resonator and radiator, as well as the length and width of the radiator, balanced the magnitude of the orthogonal modes. Finally, these structures are integrated to realize a total electrical field that accomplishes linear polarization or CP using a single port.

In the case of CP, the magnitude of the two electrical fields must be equal, as in (2), and the phase difference, δ_{L}, is 90° and −90° for left- and right-hand CPs, respectively. The equivalence between the two-magnitude e-fields in this method is determined by the ratio of the radiator's length (L_{p}) and width (W_{p}), while in the conventional filtering antenna, the ratio between L_{p} and W_{p} determines the radiator's radiation quality (Q_{rad}), which should be equal to the external quality (Q_{ext}) of the resonator. In the proposed method, the antenna–filter integration is applied by steering the ratio of W_{p} and L_{p} near 1, implying that Q_{rad} is not always equal to Q_{ext}. Besides the equal magnitude between the orthogonal e-fields, we have to provide a 90° phase delay between E_{θ} and E_{Φ} by increasing the radiator and resonator gap (C_{B}), thereby weakening E_{θ}. To maintain an equal ratio between the two fields, E_{θ} is strengthened by nearly equalizing W_{p} and L_{p} size while maintaining the same resonance frequency.

Previous studies have validated that W_{p} and L_{p} size and the gap between the orthogonal resonators are the main variables determining the polarization [30], [31], [32]. As shown in Fig. 2(a) and (b), the two designs based on

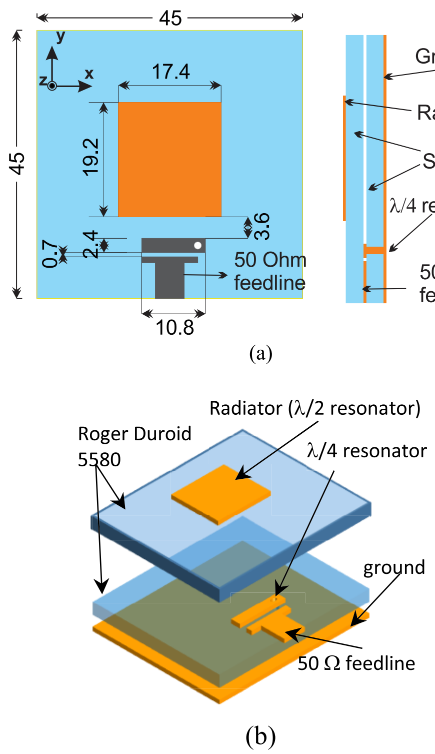

Fig. 4. (a) Geometry and side view of Antenna I with unit dimension in mm and (b) 3-D-view.

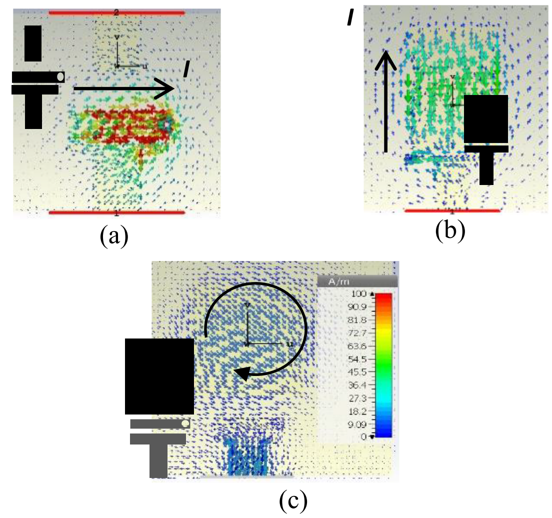

Fig. 5. Two individual structures comprising. (a) Interdigital with hole extracted using two ports with a horizontal surface current (I). (b) Rectangular radiator with coupled feed that has a vertical surface current. (c) Integration of two previous structures for left-hand circularly polarized filtering antenna. All structures resonant at 4.65 GHz.

the third- and second-order filters using a narrow rectangular radiator, resulted in impure vertical polarization [32]. Meanwhile, Fig. 3(a) shows that using wider W_{p} than the two previous designs introduces stronger magnitude e-field in the $\hat{\theta}$-direction and thus pulls the polarization to impure 75° slant. Furthermore, in Fig. 3(b), removing the gap between the radiator and interdigital resonator followed by equalizing the e-field in $\hat{\phi}$ and $\hat{\theta}$ with widening W_{p}, forms 45° polarization [31].

Section II presents an antenna–filter integration adaptation to excite circularly polarized filtering antenna using two orthogonal resonators to validate the proposed method.

III. Antenna–Filter Integration

A. Antenna Geometry

This section presents a geometric structure of the optimized filtering antenna using a new method for CP excitation. The design uses the second-order antenna–filter integration and focuses on CP excitation. The geometric structure of the filtering antenna, as shown in Fig. 4(a), comprises a 17.4 × 19.2 mm rectangular patch radiator proximity coupled with an $\lambda/4$ resonator. The gap between the rectangular radiator and the resonator (C_{B}) is 3.6 mm. The width of the $\lambda/4$ resonator is 2.4 mm, and the approximated length of $\lambda_g/4$ is 10.8 mm; it is also coupled with 50-Ω transmission lines using a 0.7-mm gap. To generate a horizontal surface current, a through hole of 1.2 mm diameter is attached on the left arm of the resonator. The antenna is printed on a 45 × 45 mm double-layer Roger Duroid 5880 substrate with a thickness of 1.575 mm and a permittivity of 2.2. Fig. 4(b) shows the two-layer antenna (3-D view), comprising of a radiator printed on the first substrate, resonator, and 50-Ω feedline on the second substrate, and ground at the bottom.

B. Design Process

First, we realize this design starting from the conventional filtering antenna extraction method to obtain the resonance frequency. The resonator and radiator as the first and second mode generator, respectively, are extracted using two ports and they must have a matching resonant. As shown in Fig. 5(a), the first mode generator is embodied by the resonator's surface current along the x-axis. This current flows from the open circuit resonator's arm to the short circuit resonator's arm. The rectangular radiator's surface current initially generates a vertical surface current along the y-axis as the second mode, as shown in Fig. 5(b). These two modes are integrated by adapting the antenna–filter integration and using the appropriate rectangular radiator size to obtain CP, as shown in Fig. 5(c). The designs of the conventional filtering antenna (Ant I) and the proposed method (Ant II) are compared to prove the novelty of the new method. All design simulations and investigations are performed using CST (computer simulation technology studio suite) tools.

The conventional filtering antenna is designed based on a second-order Chebyshev filter with 4.65-GHz operational frequency, 0.1-dB ripple, 4.7% fractional bandwidth, as well as the low-pass parameters of $g_o = 1$, $g_1 = 0.843$, $g_2 = 0.622$, and $g_3 = 1.3544$. The quality external factor (Q_{ext}) and coupling ($M_{i,i+1}$) obtained using (3) and (4) are 17.8 and 0.051, respectively

$$Q_{\mathrm{ext}} = \frac{g_n g_{n+1}}{FBW} \tag{3}$$

$$M_{i,i+1} = \frac{FBW}{\sqrt{g_i g_{i+1}}} \tag{4}$$

$$Q_{\mathrm{rad}} = \frac{f_o}{\Delta f}. \tag{5}$$

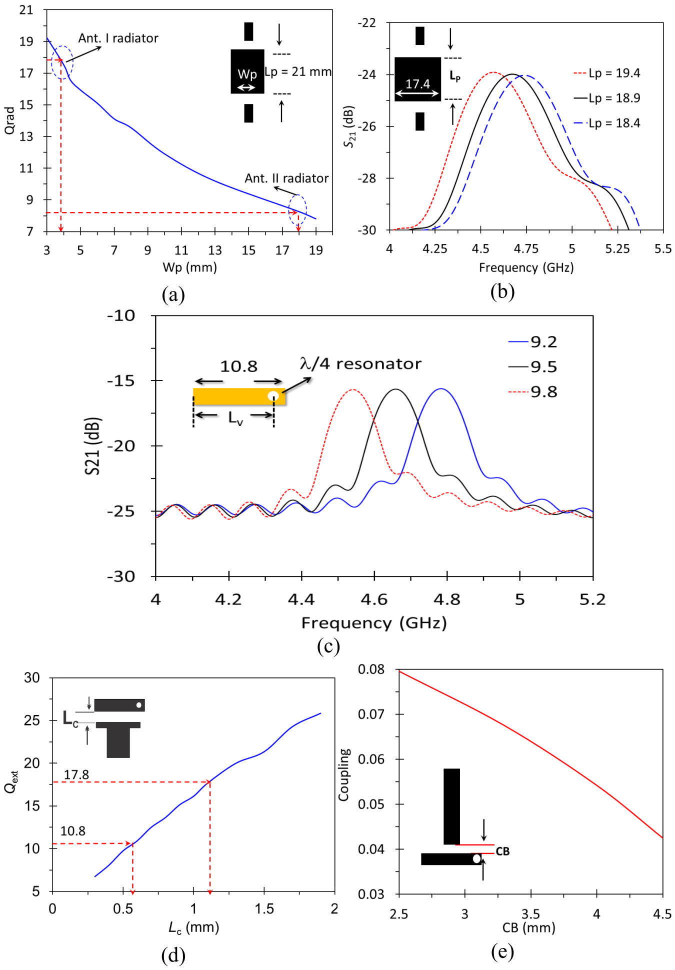

Fig. 6. (a) $Q_{\rm rad}$ with the variation in $W_{\rm p}$. (b) $L_{\rm p}$ variations with $W_{\rm p} = 17.4$ under different resonance conditions. (c) $\lambda/4$ frequency resonant with various $L_{\rm v}$. (d) $Q_{\rm ext}$ with variation in $L_{\rm c}$ [31]. (e) Coupling with various $C_{\rm B}$ (unit dimensions in mm).

The rectangular radiator is extracted using (5) to achieve $Q_{\rm rad}$, where Δf is 3-dB bandwidth and $f_{\rm o}$ is the center frequency.

The rectangular patch dimension described in Fig. 6(a) shows that 4.65-GHz resonance can be achieved using two $L_{\rm p} \times W_{\rm p}$ variations. The difference between these variations is the value of $Q_{\rm rad}$. If the ratio of $L_{\rm p}$ to $W_{\rm p}$ is close to one, $Q_{\rm rad}$ will be decreased and reversed. Based on the extraction of conventional filtering antenna, Ant I's $Q_{\rm rad}$ should be 17.8, with $L_{\rm p} \times W_{\rm p}$ around 21 × 4 mm. However, the ratio between $L_{\rm p}$ and $W_{\rm p}$ is steered to be equal using the proposed method in Ant II, as shown in Section II. Then, we used an $L_{\rm p} \times W_{\rm p}$ of 19 × 18 mm, which resonates at 4.65 GHz with $Q_{\rm rad}$ of 8.3 to balance the E_θ and E_Φ strength. A parametric study of $L_{\rm p}$ variations to

$$M_{n,n+1} = \frac{f_{n+1}^2 - f_n^2}{f_{n+1}^2 + f_n^2} \qquad (6)$$

obtains 4.65-GHz resonance, which is shown in Fig. 6(b). The $\lambda/4$ resonance frequency extraction is performed similar to [31], where the length of the resonator and through-hole position ($L_{\rm v}$) are used to determine the resonant frequency.

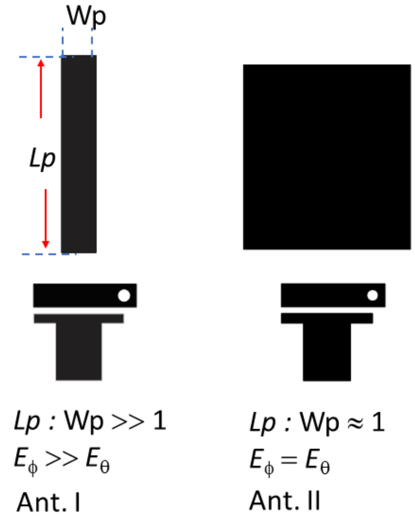

Fig. 7. Filtering antenna, Antenna I based on the second-order filter with vertical polarization and Antenna II adapting second-order filter with CP.

The $\lambda/4$ resonator obtains a 4.65-GHz resonant using a 10.8-mm arm's length with 9.5-mm $L_{\rm v}$, as shown in Fig. 6(c).

$Q_{\rm ext}$ of 17.8 is obtained when the gap between the $\lambda/4$ resonator and coupled feed ($L_{\rm c}$) is near 1.1 mm using the conventional filtering antenna extraction method for Ant I, as shown in Fig. 6(d). The gap between the resonator and patch radiator ($C_{\rm B}$) is ∼4.3 mm to obtain a 0.051 coupling using (6), as shown in Fig. 6(e), while for Ant II, $L_{\rm c}$ is set to be minimum to strengthen E_θ, and $C_{\rm B}$ is set to provide a 90° phase difference between E_θ and E_Φ. Different from the conventional filtering antenna design in Ant I that performs external quality between the resonator and the coupled feed, in Ant II, we set $L_{\rm c}$ in a range of 0.5–0.8 mm because this distance does not significantly affect polarization. However, it affects the S_{11} response; thus, we need this parameter to adjust the impedance.

IV. Results and Discussion

This section discusses the comparison results of the conventional filtering antenna represented by Ant I and the newly proposed method represented by Ant II. The S_{11} and gain response of both designs are compared to the conventional antenna without filtering structure to understand the effect of the resonator addition and the new proposed method novelty. The parametric study and the measurement results of Ant II are presented to validate the proposed method.

A. Comparison Results of Ants I and II

Applying the above procedure, we obtain an optimized design of the conventional and circularly polarized filtering antenna. Fig. 7 shows the schematic design of the two filtering antennas. The conventional filtering antenna represented by Ant I has a narrower $W_{\rm p}$ than Ant II and a marginally longer $L_{\rm p}$ than Ant II. Fig. 8 shows the S_{11} and gain response of both designs. The S_{11} response in Ant I represents the second-order filter with two returns to zero and a single peak, whereas S_{11} of the proposed method in Ant II has a single

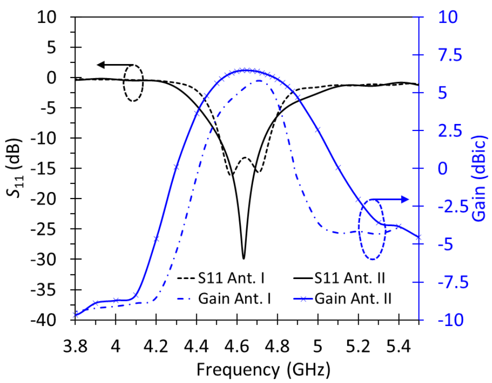

Fig. 8. Simulation of S_{11} and gain result for both designs.

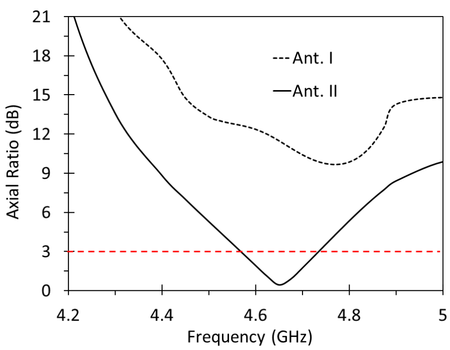

Fig. 9. AR results of Ants I and II.

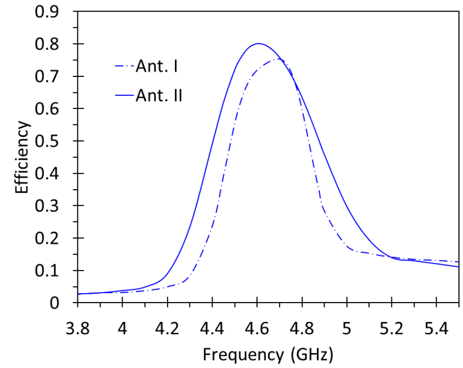

Fig. 10. Efficiency of Ants I and II.

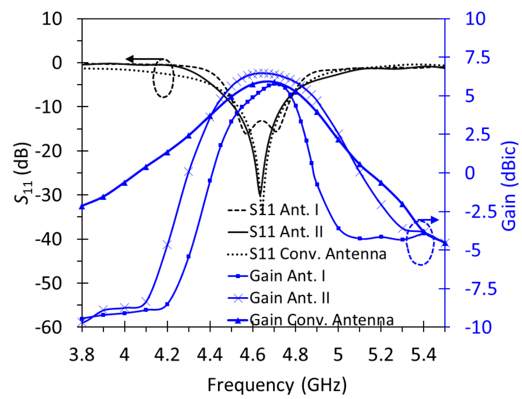

Fig. 11. S_{11} and gain parameter comparison of Ants I and II to the conventional antenna.

resonant, as in a conventional antenna. This result is due to Ant II's omitted filtering antenna procedure, which should have a certain coupling value (0.051) between the radiator and the resonator. The Q_{ext} and Q_{rad} equalizations in Ant II were also excluded, resulting in the S_{11} filtering antenna with only a single minimal response.

Both antennas' center frequency is 4.65 GHz, and the -10-dB bandwidth impedance is 246 and 224 MHz for Ants I and II, respectively. Ant I achieves its fractional bandwidth of 5.2% or 0.5% wider than the target value and two minimum S_{11} values of -16 dB at 4.57 GHz and -15.6 dB at 4.7 GHz. Ant II obtains the 4.8% fractional bandwidth with an S_{11} minimum value of -24.4 dB at 4.634 GHz. The gain response of Ant I shows a lower peak value but sharper shape than that in Ant II, and this is because the conventional extraction mainly focuses on the antenna's selectivity. A maximum gain of 5.77 dBi is achieved at 4.7 GHz for Ant I, whereas Ant II shows a maximum gain of 6.46 dBi at 4.65 GHz or 0.69 dBi higher than the previous design. Fig. 9 shows that Ant 1 does not generate CP from its high AR; in contrast, Ant II shows a 3-dB AR bandwidth of 150 MHz in a range of 4.575–4.725 GHz and attains the lowest value of 0.45 dB at 4.65 GHz. The radiator's width affects the efficiency of both antennas, where Ant I with the narrower rectangular patch has less efficiency than Ant II. The Ant I's and Ant's II maximum efficiency is ~75% and 80%, respectively, as shown in Fig. 10, and both designs have a bandpass-filter-like response. The results of Ants I and II compared to the conventional antenna without filter integration are shown in Fig. 11. Ant I shows the sharpest gain response and widest frequency compared to Ant II and the conventional antenna. Ant II has the highest gain response among the other two designs and a sharper shape than the conventional antenna. It is proven that the resonator affects selectivity in Ant II, although it is not mainly focused on gain selectivity but also on the CP characteristic. Ant II also has equal bandwidth to the conventional antenna. Other parameters to prove the CP characteristic in Ant II, as explained in (1) and (2), are the magnitude ratio between E_θ excited from the $\lambda/4$ resonator and E_Φ excited from the rectangular radiator, as shown in Fig. 12. It shows that $|E_\theta|/|E_\Phi|$ along the bandwidth ranges between 1.7 and 1.09 or near the theoretical value of 1, whereas phase differences are between $-83°$ and $-98°$ or near the ideal value of $-90°$. Those values indicate that Ant II has a left-hand CP.

B. Parametric Study of Ant II

The response of AR under different W_p's has been proven in Ants I and II, which is heavily related to the magnitude of E_θ and E_Φ. Next, the effects of the gap spacing between the resonator and rectangular radiator (C_B) and the gap between the resonator and coupled feed are investigated in Ant II. Fig. 13 shows that in Ant II, the AR is unaffected by the gap between the resonator and coupled feed (L_c). It shows that S_{11} is optimum when L_c is 0.7 mm because, with less or more distance with an increment of 0.3 mm, its value increases; in contrast to the AR, which is unaffected by L_c. In Ant II, the gap between the radiator and the resonator (C_B) affects the AR

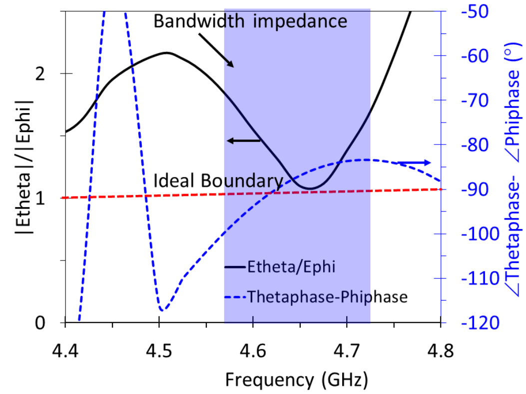

Fig. 12. Ratio magnitude E_θ to E_Φ and phase difference of Ant II.

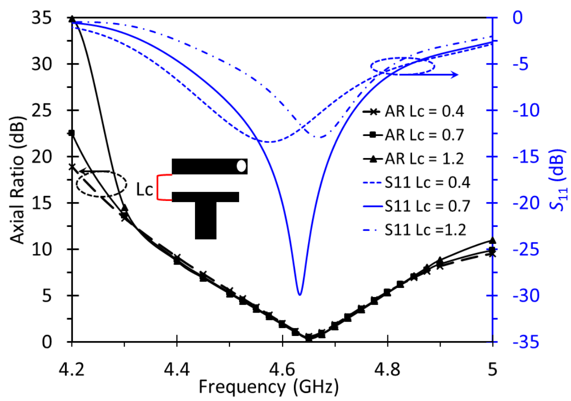

Fig. 13. AR and S_{11} response vary under different L_C's (all unit dimensions are in mm).

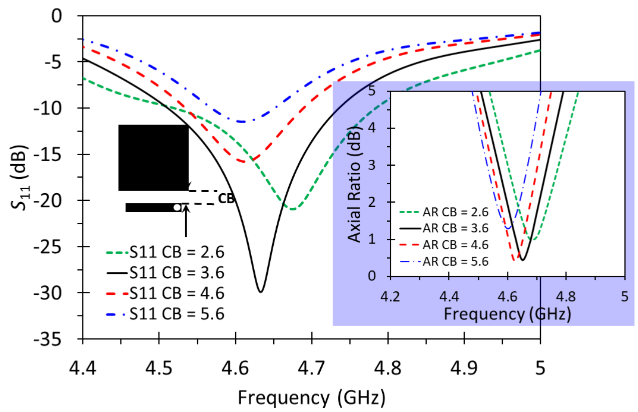

Fig. 14. AR and S_{11} response vary under different C_B's with constant W_p and L_p (all unit dimensions in mm).

and S_{11}. Fig. 14 shows that with an increment of 1 mm, the S_{11} response and AR are altered. The AR is minimum when the C_B value is 3.6 mm because, if it is less or more, the AR and S_{11} increase. All parametric studies are conducted with constant W_p and L_p. C_B is an essential parameter for differentiating 45° linear polarization and CP in the proposed method because widening C_B will contribute 90° delay, whereas minimizing C_B to 0 mm will produce 0° or 180° delay between E_θ and E_Φ, as performed in [31].

C. Measurement Result

To validate the proposed method, Ant II is fabricated and measured. Fig. 15 shows the photograph consisting of the assembled antenna in Fig. 15(a), the radiator layer in Fig. 15(b), and the feeding network in Fig. 15(c). The S_{11} result is shown in Fig. 16, where the simulation and measurement results have a good agreement. The measured frequency range of the proposed circularly polarized filtering antenna with $S_{11} < -10$ dB is 4.520–4.756 GHz, which shifts to a higher frequency and 4.8% wider than the simulation result. Its S_{11} gets the lowest value of -25 dB at 4.64 GHz, which is 4 dB higher than the simulated results. The 3-dB AR bandwidth measurement results shown in Fig. 17 are 100 MHz in a range of 4.633–4.733 GHz, which is 30% narrower than the simulation result. The lowest AR is better than the simulation by 0.33 dB but shifts to 4.68 GHz. The insignificant discrepancy between the measured and simulated results is attributed to the assembly and fabrication tolerance. The gain measurement result depicted in Fig. 18 shows a

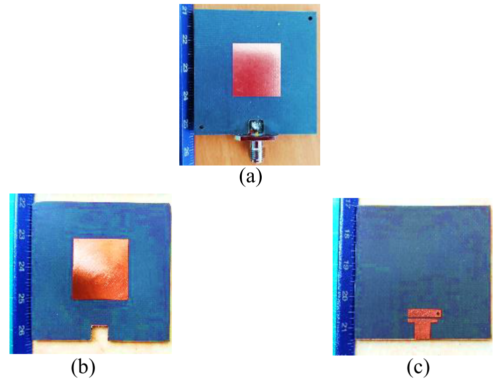

Fig. 15. Photograph of Ant II. (a) Integrated layers. (b) Radiator patch. (c) Feeding structure.

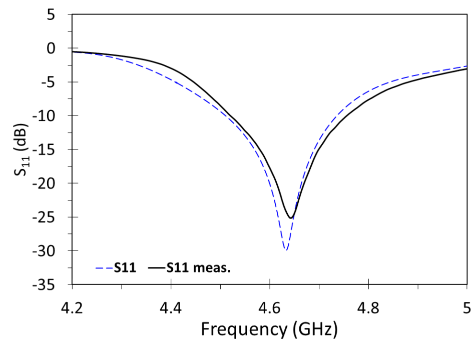

Fig. 16. S_{11} measurement result of Ant II.

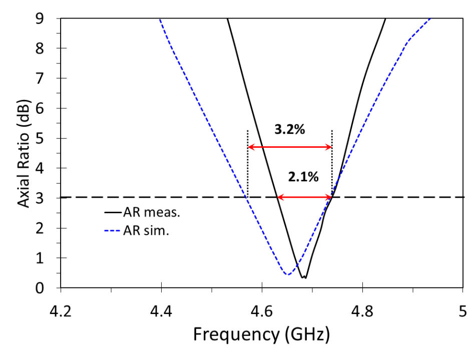

Fig. 17. AR measurement result of Ant II at $\varphi = 0°$ and $\theta = 0°$.

TABLE I
COMPARISON WITH PREVIOUS CP FILTERING ANTENNA

Ref.	Profile	CP Method	Delay/filtering circuit	Gain (dBic)	ARBW (%)
[3]	0.57λ×0.6125λ×0.006λ	Single feed line with truncated radiator	Extra circuit	2.1–2.8	20.5
[12]	0.77λ×0.77λ×0.03λ	Single feed line with truncated radiator	Extra circuit	8	8.5
[13]	0.91λ×0.91λ×0.022λ	Single feed line with radiator perturbation	Extra circuit	8.3	5.3
[14]	1λ×1λ×0.036λ	Single feed line with radiator perturbation	Extra circuit	8	3.9
[16]	0.53λ×0.53λ×0.07λ	Orthogonal feedlines	Extra circuit	5.2	12.5
[17]	1.06λ×1.06λ×0.027λ	Orthogonal feedlines	Extra circuit	5.8	8.8
[18]	0.72λ×0.72λ×0.018λ	Orthogonal feedlines	Extra circuit	6.1	3.8
This work	0.69λ×0.69λ×0.048λ	Single feedline with orthogonal resonators	No extra circuit	6.72	3.2

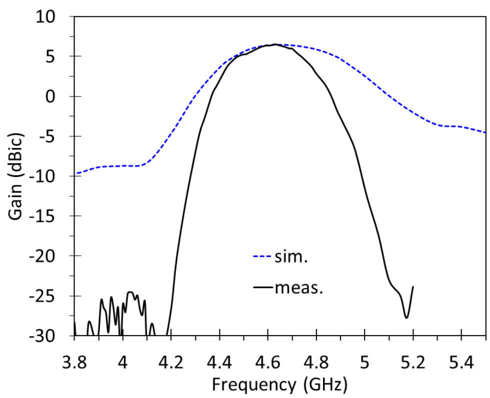

Fig. 18. Gain measurement of Ant II.

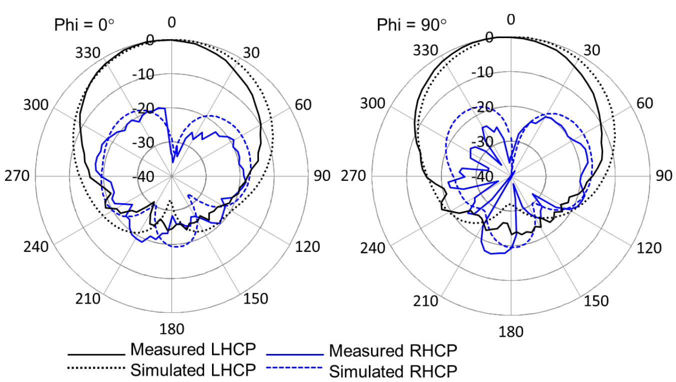

Fig. 19. Normalized radiation pattern Ant II at 4.68 GHz.

bandpass response along the bandwidth with a maximum value of 6.7 dBi at 4.65 GHz or 0.3 dB higher than the simulation result. The selectivity at the lower frequency is better than the upper frequency.

The measurement gain shows a sharper response than the simulation since the simulation gain samples did not capture the dips that always arise in the filtering antenna measurement. The normalized radiation pattern measurement at 4.68 GHz is shown in Fig. 19. It shows a unidirectional pattern with the main lobe direction at 0° and −3-dB beamwidth of 80.5° and 81.5° at $\varphi = 0°$ and 90°, respectively. The cross-polarization discriminant in the main lobe is higher than 30 dB for $\varphi = 0°$ and 90°, which agrees well with the simulation results.

Table I compares the proposed and previous methods, demonstrating that using a single feedline with an orthogonal resonator eliminates the need for an additional delay and filtering circuit. Cheng and Li [3] employed a single feedline with circular radiator perturbation, having the broadest AR bandwidth because it used a dipole antenna and a tradeoff with the lowest gain. The highest gain value was obtained in [12], [13], and [14] using truncated radiator or radiator perturbation but with compensation for the size of the antennas. Some previous studies used two orthogonal feedlines to produce a broader AR bandwidth than the proposed method [16], [17], [18]. Although the proposed method had the narrowest AR bandwidth, it had the highest gain without extra circuit to produce CP and selectivity. Furthermore, we are optimistic that we can improve the AR bandwidth in the future research using antenna–filter integration that can control the bandwidth.

V. CONCLUSION

A new method for developing a circularly polarized antenna adopting a second-order filtering antenna has been demonstrated. The integration of orthogonal surface current in the rectangular radiator and $\lambda/4$ resonator resulted in a left-hand CP filtering antenna. The radiator's length and width significantly affected the electric field magnitude in the θ and Φ-directions. The gap spacing between the rectangular radiator and $\lambda/4$ resonator determined the phase delay. The performance of the conventional filtering antenna and the antenna based on the new method was compared. The proposed method was validated by the agreement between the simulation and measurement results.

ACKNOWLEDGMENT

The authors would like to thank Anshari and Rosza from the Research Center for Satellite Technology, National Research and Innovation Agency, Kevin, Nathan, Dian, and Galih from the Electrical Engineering Department, Universitas Indonesia, for their support in the measurements; Telecommunication Laboratory, Electrical Engineering Department, Faculty of Engineering, Universitas Indonesia, for providing the measurement laboratory and CST software; and Arry Yanuar for assisting with data sorting.

References

[1] F. N. Ayoub, Y. Tawk, E. Ardelean, J. Costantine, S. A. Lane, and C. G. Christodoulou, "Cross-slotted waveguide array with dual circularly polarized radiation at W-band," *IEEE Trans. Antennas Propag.*, vol. 70, no. 1, pp. 268–277, Jan. 2022, doi: 10.1109/TAP.2021.3090863.

[2] E. T. Rahardjo, S. Kitao, and M. Haneishi, "Circularly polarized planar antenna excited by cross-slot coupled coplanar waveguide feedline," in *IEEE Antennas Propag. Soc., AP-S Int. Symp. Dig.*, vol. 3, Jun. 1994, pp. 2220–2223, doi: 10.1109/aps.1994.408042.

[3] W. Cheng and D. Li, "Circularly polarised filtering monopole antenna based on miniaturised coupled filter," *Electron. Lett.*, vol. 53, no. 11, pp. 11–12, 2017, doi: 10.1049/el.2017.1094.

[4] T. Li and X. Gong, "Vertical integration of high-Q filter with circularly polarized patch antenna with enhanced impedance-axial ratio bandwidth," *IEEE Trans. Antennas Propag.*, vol. 66, no. 6, pp. 3119–3128, Jun. 2018, doi: 10.1109/TMTT.2018.2832073.

[5] N. Hussain, M. Jeong, A. Abbas, and N. Kim, "Metasurface-based single-layer wideband circularly polarized MIMO antenna for 5G millimeter-wave systems," *IEEE Access*, vol. 8, pp. 130293–130304, 2020, doi: 10.1109/ACCESS.2020.3009380.

[6] C. E. Santosa, J. T. S. Sumantyo, S. Gao, and K. Ito, "Broadband circularly polarized microstrip array antenna with curved-truncation and circle-slotted parasitic," *IEEE Trans. Antennas Propag.*, vol. 69, no. 9, pp. 5524–5533, Sep. 2021, doi: 10.1109/TAP.2021.3060122.

[7] S. Maddio, G. Pelosi, and S. Selleri, "Circularly polarised sequential array with enhanced gain and bandwidth for applications in C-band," *IET Microw., Antennas Propag.*, vol. 14, no. 15, pp. 1926–1932, Dec. 2020, doi: 10.1049/iet-map.2020.0450.

[8] M. K. Ray, K. Mandal, N. Nasimuddin, A. Lalbakhsh, R. Raad, and F. Tubbal, "Two-pair slots inserted CP patch antenna for wide axial ratio beamwidth," *IEEE Access*, vol. 8, pp. 223316–223324, 2020, doi: 10.1109/ACCESS.2020.3043406.

[9] L. Wang and Y.-F. En, "A wideband circularly polarized microstrip antenna with multiple modes," *IEEE Open J. Antennas Propag.*, vol. 1, pp. 413–418, 2020, doi: 10.1109/OJAP.2020.3009884.

[10] U. Ullah, M. Al-Hasan, S. Koziel, and I. B. Mabrouk, "Series-slot-fed circularly polarized multiple-input–multiple-output antenna array enabling circular polarization diversity for 5G 28 GHz indoor applications," *IEEE Trans. Antennas Propag.*, vol. 69, no. 9, pp. 5607–5616, Sep. 2021, doi: 10.1109/TAP.2021.3066247.

[11] C. Zhou, B. Wang, and H. Wong, "A compact dual-mode circularly polarized antenna with frequency reconfiguration," *IEEE Antennas Wireless Propag. Lett.*, vol. 20, no. 6, pp. 1098–1102, Jun. 2021, doi: 10.1109/LAWP.2021.3073417.

[12] Y. Dong et al., "Broadband circularly polarized filtering antennas," *IEEE Access*, vol. 6, pp. 76302–76312, 2018, doi: 10.1109/ACCESS.2018.2883494.

[13] W.-J. Yang, Y.-M. Pan, and X.-Y. Zhang, "A single-layer low-profile circularly polarized filtering patch antenna," *IEEE Antennas Wireless Propag. Lett.*, vol. 20, no. 4, pp. 602–606, Apr. 2021.

[14] S. Ji, Y. Dong, Y. Pan, Y. Zhu, and Y. Fan, "Planar circularly polarized antenna with bandpass filtering response based on dual-mode SIW cavity," *IEEE Trans. Antennas Propag.*, vol. 69, no. 6, pp. 3155–3164, Jun. 2021, doi: 10.1109/TAP.2020.3037819.

[15] M. K. Khandelwal, S. Kumar, and B. K. Kanaujia, "Design, modeling and analysis of dual-feed defected ground microstrip patch antenna with wide axial ratio bandwidth," *J. Comput. Electron.*, vol. 17, no. 3, pp. 1019–1028, Sep. 2018, doi: 10.1007/s10825-018-1173-1.

[16] Z. H. Jiang and D. H. Werner, "A compact, wideband circularly polarized co-designed filtering antenna and its application for wearable devices with low SAR," *IEEE Trans. Antennas Propag.*, vol. 63, no. 9, pp. 3808–3818, Sep. 2015, doi: 10.1109/TAP.2015.2452942.

[17] Q.-S. Wu, X. Zhang, and L. Zhu, "Co-design of a wideband circularly polarized filtering patch antenna with three minima in axial ratio response," *IEEE Trans. Antennas Propag.*, vol. 66, no. 10, pp. 5022–5030, Oct. 2018, doi: 10.1109/TAP.2018.2856104.

[18] W. Wang, C. Chen, S. Wang, and W. Wu, "Circularly polarized patch antenna with filtering performance using polarization isolation and dispersive delay line," *IEEE Antennas Wireless Propag. Lett.*, vol. 19, no. 8, pp. 1457–1461, Aug. 2020.

[19] H. Wenjia and Y. Horii, "Enhanced group delay of microstrip-line-based dispersive delay lines with LC resonant circuits for real-time analog signal processing," in *Proc. IEEE Asia Pacific Microw. Conf. (APMC)*, Nov. 2017, pp. 273–275.

[20] R. Kumar and K. J. Vinoy, "Large group delay in microstrip circuit using coupled open stubs and collocated ground slots," *IEEE Microw. Wireless Compon. Lett.*, vol. 30, no. 6, pp. 553–556, Jun. 2020, doi: 10.1109/LMWC.2020.2992104.

[21] Z. Wang, Y. Meng, S. Fang, and H. Liu, "Wideband flat negative group delay circuit with improved signal attenuation," *IEEE Trans. Circuits Syst. II, Exp. Briefs*, vol. 69, no. 8, pp. 3371–3375, Aug. 2022, doi: 10.1109/TCSII.2022.3156537.

[22] G. Chaudhary and Y. Jeong, "Synthesis of reflection-type coupled line all-pass circuit with arbitrary prescribed wideband flat group delay," *IEEE Microw. Wireless Compon. Lett.*, vol. 27, no. 10, pp. 876–878, Oct. 2017, doi: 10.1109/LMWC.2017.2747149.

[23] B. Ravelo, "Negative group-delay phenomenon analysis with distributed parallel interconnect line," *IEEE Trans. Electromagn. Compat.*, vol. 58, no. 2, pp. 573–580, Apr. 2016, doi: 10.1109/TEMC.2016.2516899.

[24] T. Shao, Z. Wang, S. Fang, H. Liu, and Z. N. Chen, "A full-passband linear-phase band-pass filter equalized with negative group delay circuits," *IEEE Access*, vol. 8, pp. 43336–43343, 2020, doi: 10.1109/ACCESS.2020.2977100.

[25] T. Zhang, T. Yang, and P.-L. Chi, "Novel reconfigurable negative group delay circuits with independent group delay and transmission loss/gain control," *IEEE Trans. Microw. Theory Techn.*, vol. 68, no. 4, pp. 1293–1303, Apr. 2020, doi: 10.1109/TMTT.2019.2955704.

[26] M. K. Mandal, D. Deslandes, and K. Wu, "Complementary microstrip-slotline stub configuration for group delay engineering," *IEEE Microw. Wireless Compon. Lett.*, vol. 22, no. 8, pp. 388–390, Aug. 2012, doi: 10.1109/LMWC.2012.2205229.

[27] M. L. N. Chen, L. J. Jiang, and W. E. I. Sha, "Artificial perfect electric conductor-perfect magnetic conductor anisotropic metasurface for generating orbital angular momentum of microwave with nearly perfect conversion efficiency," *J. Appl. Phys.*, vol. 119, no. 6, pp. 1–5, 2016.

[28] Q.-S. Wu, X. Zhang, and L. Zhu, "A feeding technique for wideband CP patch antenna based on 90° phase difference between tapped line and parallel coupled line," *IEEE Antennas Wireless Propag. Lett.*, vol. 18, no. 7, pp. 1468–1471, Jul. 2019.

[29] Q.-S. Wu, X. Zhang, and L. Zhu, "A wideband circularly polarized patch antenna with enhanced axial ratio bandwidth via co-design of feeding network," *IEEE Trans. Antennas Propag.*, vol. 66, no. 10, pp. 4996–5003, Oct. 2018, doi: 10.1109/TAP.2018.2851616.

[30] D. A. Cahyasiwi, F. Y. Zulkifli, and E. T. Rahardjo, "Stacked interdigital filtering antenna with slant polarization," in *Proc. IEEE Conf. Antenna Meas. Appl. (CAMA)*, Oct. 2019, pp. 275–278.

[31] D. A. Cahyasiwi, F. Y. Zulkifli, and E. T. Rahardjo, "Switchable slant polarization filtering antenna using two inverted resonator structures for 5G application," *IEEE Access*, vol. 8, pp. 224033–224043, 2020, doi: 10.1109/ACCESS.2020.3043824.

[32] D. A. Cahyasiwi, E. Roza, M. Mujirudin, N. M. Nashuha, F. Y. Zulkifli, and E. T. Rahardjo, "Selectivity improvement of interdigital filtering-antenna using different orders for 5G application," *Int. J. Microw. Wireless Technol.*, pp. 1–9, Nov. 2022, doi: 10.1017/S1759078722001143.

[33] W. Stutzman and G. Thiele, *Antenna Theory and Design*, 3rd ed. Hoboken, NJ, USA: Wiley, 2013.

Dwi Astuti Cahyasiwi (Member, IEEE) received the bachelor's, Magister, and Ph.D. degrees in electrical engineering from Universitas Indonesia, Depok, Indonesia, in 1997, 2009, and 2022, respectively.

She received an Excellent Scholarship for Indonesia's Lecture (Beasiswa Unggulan Dosen Indonesia/BUDI-LPDP) for the Ph.D. degree. She has been a Lecturer with the Electrical Engineering Department, Universitas Muhammadiyah Prof. Dr. HAMKA, since 2000. Her research interests include the integration design of antenna and filter, multiple-input–multiple-output (MIMO) antenna, dual-polarized antenna systems, metasurface, polarization converter, and microwave circuits.

Dr. Cahyasiwi has been a member of the IEEE Antenna and Propagation Society (AP-S) since 2021 and a Reviewer of IEEE ACCESS since 2020. She was a recipient of the Best Student Paper Award at the 2019 IEEE Conference on Antenna Measurement and Applications (CAMA).

Fitri Yuli Zulkifli (Senior Member, IEEE) received the bachelor's in electrical engineering from Universitas Indonesia (UI), Depok, Indonesia, in 1997, the M.Sc. degree from the Karlsruhe Institute of Technology, Karlsruhe, Germany, in 2002, and the Ph.D. degrees in electrical engineering from UI in 2009.

She joined the Antenna Propagation and Microwave Research Group (AMRG), UI, in 1997 and has been a Lecturer with the Electrical Engineering Department, UI, since 1998. Since 2017, she has been a Professor in antenna and microwave engineering. She has published more than 200 papers in journals/conference proceedings and received more than 40 research grants. She now leads "Laboratory Prof. Fitri Yuli Zulkifli" and also the Head of the Professional Engineering Study Program with UI. Her research interests include antenna, propagation, microwave, and in the field of telecommunication.

Prof. Zulkifli became the Joint Chapter Chair of Microwave Theory and Techniques (MTT)/AP Indonesia from 2011 to 2012. From 2017 to 2018, she was the IEEE Indonesia Section Chair, and from 2019 to 2022, she has been serving as a Committee Member for the R10 Conference and Technical Seminar and Conference Quality Management. In 2023 she is a member of Technical Program Integrity Committee (TPIC) and also R10 Conference Quality Management.

Eko Tjipto Rahardjo (Member, IEEE) was born in Pati, Indonesia, in April 1958. He received the Ir. (Insinyur) degree from Universitas Indonesia, Depok, Indonesia, in 1981, the M.S. degree from the University of Hawai'i at Manoa, Honolulu, HI, USA, in 1987, and the Ph.D. degree from Saitama University, Urawa, Japan, in 1996, all in electrical engineering.

Since 1982, he has been a Teaching Assistant with the Department of Electrical Engineering, Universitas Indonesia. Since 2005, he has been appointed as a Professor of electrical engineering. He was the Chairperson of the University Senate, Universitas Indonesia, from 2011 to 2012; the Head of the Department of Electrical Engineering, Universitas Indonesia, from 2004 to 2008; and the Executive Director of the Quality Undergraduate Education (QUE), Department of Electrical Engineering, Universitas Indonesia, from 1999 to 2004, where he was also the Head of the Telecommunication Laboratory from 1997 to 2004. Since 2003, he has been the Director of the Antenna Propagation and Microwave Research Group (AMRG), Universitas Indonesia. He has published and presented more than 100 research articles in national and international journals and symposiums. His research interests include antenna engineering, wave propagation, microwave circuits, communication systems, and telecommunications system regulation.

Prof. Rahardjo is a member of the IEEE Antenna and Propagation Society (AP-S) and the IEEE Microwave Theory and Technique Society (MTTS). He has been a member of the International Steering Committee (ISC) of the Asia–Pacific Microwave Conference (APMC) since 2010 and the International Advisory Board of the International Symposium on Antenna and Propagation (ISAP) since 2012. He received an Indonesian Government Scholarship through Mid-west Universities Concortium for International Activities (MUCIA) from 1984 to 1987, a Hitachi Scholarship from 1992 to 1996, a Young Researcher's Award from Universitas Indonesia in 1996, a Second Winner of the Best Researcher Award in Science and Technology from Universitas Indonesia in 2009, and a Second Winner of Best Teaching Award from Universitas Indonesia in 2010. He was the Founder of the IEEE Joint Chapter Microwave Theory and Techniques (MTT-S)/AP-S, Indonesia. He served as the President for the IEEE Joint Chapter MTT-S/AP-S from 2009 to 2010 and the IEEE Indonesia Section from 2014 to 2015. He was the General Chairperson of the Indonesia Malaysia Microwave and Antenna Conference (IMMAC), Depok, in 2010, and the Indonesia–Japan Joint Scientific Symposium (IJJSS), Bali, in 2010; and the General Co-Chairperson of the Indonesia–Japan Joint Scientific Symposium (IJJSS), Chiba, Japan, in 2012. In addition, he was the General Chair of the First Indonesia–Japan Workshop on Antennas and Wireless Technology (IJAWT), Depok, in 2017, and the 2019 IEEE International Conference on Antenna Measurements and Applications (CAMA), Bali, in October 2019.